

See discussions, stats, and author profiles for this publication at: <https://www.researchgate.net/publication/40732454>

Efficient Intramolecular Charge Transfer in Oligoyne-Linked Donor- π -Acceptor Molecules

ARTICLE in CHEMISTRY - A EUROPEAN JOURNAL · DECEMBER 2009

Impact Factor: 5.73 · DOI: 10.1002/chem.200902099 · Source: PubMed

CITATIONS

27

READS

36

7 AUTHORS, INCLUDING:



Lars-Olof Palsson Dr

Durham University

71 PUBLICATIONS 1,944 CITATIONS

SEE PROFILE



S. M. King

Durham University

29 PUBLICATIONS 638 CITATIONS

SEE PROFILE



Andrew Beeby

Durham University

192 PUBLICATIONS 6,600 CITATIONS

SEE PROFILE



Andy Monkman

Durham University

416 PUBLICATIONS 9,794 CITATIONS

SEE PROFILE

Efficient Intramolecular Charge Transfer in Oligoyne-Linked Donor- π -Acceptor Molecules

Lars-Olof Pålsson,^{*,[a]} Changsheng Wang,^[a] Andrei S. Batsanov,^[a] Simon M. King,^[b]
Andrew Beeby,^[a] Andrew P. Monkman,^[b] and Martin R. Bryce^{*,[a]}

Abstract: Studies are reported on a series of triphenylamine-(C \equiv C)_n-2,5-diphenyl-1,3,4-oxadiazole dyad molecules ($n=1-4$, **1**, **2**, **3** and **4**, respectively) and the related triphenylamine-C₆H₄-(C \equiv C)₃-oxadiazole dyad **5**. The oligoyne-linked D- π -A (D=electron donor, A=electron acceptor) dyad systems have been synthesised by palladium-catalysed cross-coupling of terminal alkynyl and butadiynyl synthons with the corresponding bromoalkynyl moieties. Cyclic voltammetric studies reveal a reduction in the HOMO-LUMO gap in the series of compounds **1-4** as the oligoyne chain length increases, which is consistent with ex-

tended conjugation through the elongated bridges. Photophysical studies provide new insights into conjugative effects in oligoyne molecular wires. In non-polar solvents the emission from these dyad systems has two different origins: a locally excited (LE) state, which is responsible for a $\pi^*\rightarrow\pi$ fluorescence, and an intramolecular charge transfer (ICT) state, which produces charge-transfer emission. In polar solvents the LE state emission vanishes

and only ICT emission is observed. This emission displays strong solvatochromism and analysis according to the Lippert-Mataga-Oshika formalism shows significant ICT for all the luminescent compounds with high efficiency even for the longer more conjugated systems. The excited-state properties of the dyads in non-polar solvents vary with the extent of conjugation. For more conjugated systems a fast non-radiative route dominates the excited-state decay and follows the Engelman-Jortner energy gap law. The data suggest that the non-radiative decay is driven by the weak coupling limit.

Keywords: charge transfer • fluorescence • oligoynes • oxadiazole • photodynamics • triarylamine


Introduction

Charge- and electron-transfer dynamics through organic molecular wires are of major interest in chemistry, physics and biology.^[1] Important incentives for studying this topic stem from both fundamental and practical aspects, in particular:

i) the development of new materials for the emerging technologies of molecular and nanoscale electronics,^[2] and ii) understanding and mimicking key biological molecules that mediate electron-transfer processes, for example, photosynthetic reaction centres, redox proteins and nucleic acids.^[3] Many successful strategies have been developed to control and tune the magnitude of charge transfer through conjugated bridges by end capping with various organic donor and acceptor groups, that is, covalent D- π -A systems (D=electron donor, A=electron acceptor)^[4] or organometallic moieties.^[5] In these molecules the systematic variation of parameters such as the redox potentials of the end groups, free energy changes in charged states, intramolecular distances (i.e., length of the bridge), topology and relative orientations of the component units has enabled charge separation and storage characteristics to be probed in great detail by electrochemical and spectroscopic techniques. On the basis of this information, organic molecules—including oligomers and polymers^[6]—can now be tailored for specific electrical or optoelectronic applications, such as wires,^[7] switches,^[8] photovoltaic cells,^[9] electroluminescent devices,^[10] field-

[a] Dr. L.-O. Pålsson, Dr. C. Wang, Dr. A. S. Batsanov, Dr. A. Beeby, Prof. M. R. Bryce
Department of Chemistry, Durham University
Durham DH1 3LE (UK)
Fax: (+44) 191 384 4737
E-mail: lars-olof.palsson@durham.ac.uk
m.r.bryce@durham.ac.uk

[b] Dr. S. M. King, Prof. A. P. Monkman
Department of Physics, Durham University
Durham DH1 3LE (UK)

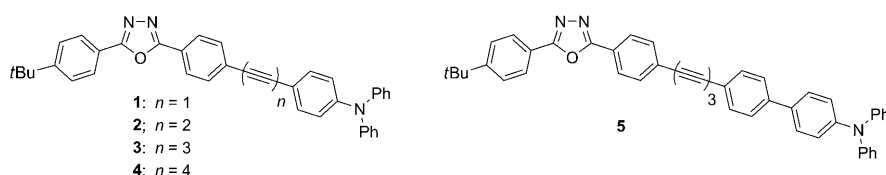
 Supporting information for this article (General experimental methods, synthetic details and characterisation data for compounds **3-5**, **7**, **8**, **10**, **13** and **14**; additional photophysical data; X-ray crystallographic data for **3**, **4**, **5** and **8** in CIF format. This material is available on the WWW under <http://dx.doi.org/10.1002/chem.200902099>.

effect transistors^[11] and single-molecule electrode junctions.^[12]

To enhance electronic communication over nanometer distances, conjugated D- π -A dyads that possess delocalised π systems and tunable HOMO-LUMO gaps are attractive targets. With sufficient overlap between the wave functions, electron transfer along the wire can be facilitated. In this context, a range of conjugated π -electron bridges have been studied. Specific examples include: oligo(*para*-phenylene)s,^[13] oligo(*para*-phenylenevinylene)s (OPVs),^[14] oligo(*para*-phenyleneethynylene)s (OPEs),^[15] oligofluorenes,^[16] oligothiophenes,^[17] oligoenes and carotenoids.^[18]

Oligoynes [(C \equiv C) $_n$] comprise an array of sp-hybridised carbon atoms with approximately cylindrical electron delocalisation along a one-dimensional, rigid-rod backbone^[19] and they have only rarely been studied as bridges in organic D- π -A systems. This is largely due to the significant synthetic challenges posed by unsymmetrical derivatives with $n > 2$.^[19d,e] To our knowledge, the only previous systematic study concerns a series of Zn-porphyrin-(C \equiv C) $_n$ -C₆₀ dyads ($n = 1-4$) in which photoinduced charge separation and charge recombination were studied as a function of D-A distance.^[20] The observed very efficient electron transfer (small attenuation factor (β) of $0.06 \pm 0.005 \text{ \AA}^{-1}$) was rationalised in terms of full π conjugation between the phenyl ring of the porphyrin donor, the oligoyne linker and the C₆₀ acceptor. Oligoynes are linear structures through which electron transport is independent of rotation around the single bonds—a feature that makes them clearly distinct from OPVs and OPEs, where the barrier to rotation around single bonds is low and conjugation is interrupted when the phenyl rings are rotated with respect to each other.^[21] Previous experimental studies of the optical properties of symmetrical silyl end-capped oligoynes ($n = 2-10$) established that they possess extensive conjugation, which was supported by theoretical models of the third-order non-linear optical response as a function of the number of alkyne units.^[22]

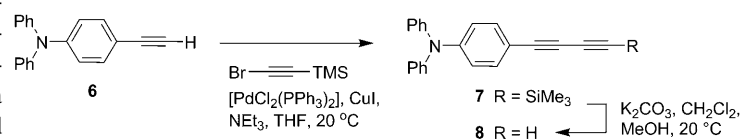
We recently described compounds **1** and **2** as part of a study on D- π -A dyads with different electron-donor moieties (D = tetrathiafulvalene (TTF), bithiophene, 9-(4,5-dimethyl-1,3-dithiol-2-ylidene)fluorene and triphenylamine) connected to electron-accepting 2,5-diphenyl-1,3,4-oxadiazole (OXD) units. The latter was chosen because of its excellent chemical and thermal stabilities and high photoluminescence quantum yield (PLQY). We established that both **1** and **2** are strongly luminescent although the PLQY was lower for **2** and it was concluded that intramolecular energy transfer was less efficient through the butadiynylene bridge (**2**) than the ethynylene bridge (**1**).^[23] Based on these initial results, we have now focused our attention on a more extensive series of triphenylamine-(C \equiv C) $_n$ -2,5-diphenyl-1,3,4-oxadiazole molecules including novel hexatriyne and octatetrayne analogues (**1**, **2**, **3** and **4**, $n = 1-4$, respectively) and



the related triphenylamine-C₆H₄-(C \equiv C)₃-diphenyloxadiazole **5** with the aim of probing their optoelectronic properties as a function of the D-A distance. This work provides new insights into conjugative effects of oligoyne bridges and, in particular, establishes that non-radiative decay in oligoynes follows the Engelman-Jortner energy gap law.^[24]

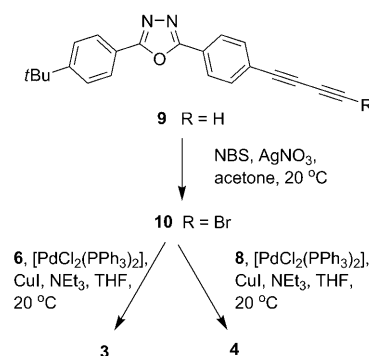
Results and Discussion

Synthesis: The general protocol for synthesising the molecules **1-5** involved palladium-catalysed cross-coupling reactions of terminal alkynes with terminal alkynyl bromides. Compound **6** reacted with 1-bromo-2-trimethylsilylacetylene (TMSA bromide) to give compound **7**, which was desilylated by using potassium carbonate in MeOH/CH₂Cl₂ at room temperature to give the terminal butadiyne reagent **8**, which was isolated as a crystalline solid (Scheme 1, 35% overall yield for the two steps).



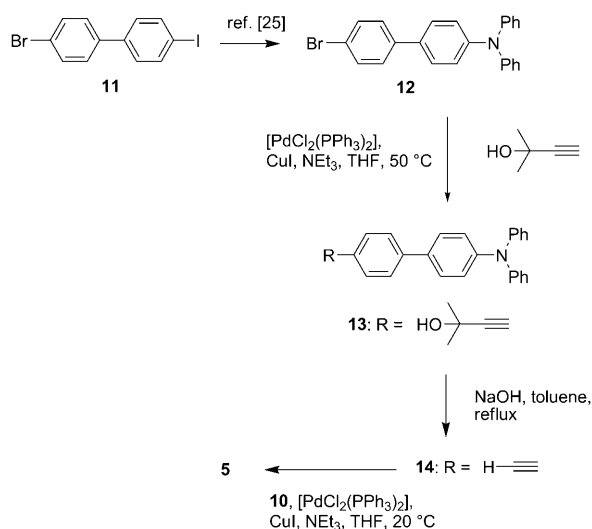
Scheme 1. Synthesis of terminal butadiyne derivative **8** (TMS = trimethylsilyl).

Compound **10** was obtained in 90% yield by bromination of **9** as shown in Scheme 2. Reactions of **10** with **6** and **8**, respectively, catalysed by [PdCl₂(PPh₃)₂]/CuI, under basic conditions gave the corresponding hexatriyne and octatetrayne products **3** and **4** in 56% and 39% yields. Scheme 3 shows



Scheme 2. Synthesis of compounds **3** and **4** (NBS = *N*-bromosuccinimide).

the synthesis of compound **5**. Compound **12**^[25] was converted into **13** for which the polar 2-hydroxy-2-propyl protecting group facilitated purification. Standard deprotection of **13** under basic conditions^[26] gave the target alkyne reagent **14** (70 % yield from the 2 steps). By analogy with the synthesis of **3**, the cross-coupling reaction of **14** with **10** gave **5** in 42 % yield.



Scheme 3. Synthesis of compound **5**.

X-ray crystallography: Single-crystal X-ray structures were determined for **3**, **4**, **5** (as a CH₂Cl₂ hemi-solvate) and **8** (Figure 1). In each case, the N3 atom has sp² geometry, with the three adjacent benzene rings inclined to its plane in a propeller-like fashion. The triyne “rod” in **3** is bent in the “symmetrical bow” fashion^[19] with an additional spiral twist. The angle between the terminal C–C bonds, θ , of 27.6° and the contraction of the overall chain length, δ , (compared to the sum of the bond lengths) of 1.4 % are rather high: of the 46 previously reported triynes^[27] only 11 have $\theta > 14^\circ$ and only one^[28] (with $\theta = 28.9^\circ$, $\delta = 1.8\%$) is bent more strongly than **3**. The tetrayne rod in **4** adopts an “asymmetric bow” bend of the magnitude ($\theta = 13.9^\circ$, $\delta = 0.5\%$) not uncommon for tetraynes with bulky, especially organometallic, end groups.^[19a,b] It can be argued that the bending is caused by incompatible packing demands of the rods and the end groups, whereas in **5** the bending is slight ($\theta = 3.8^\circ$, $\delta = 0.2\%$) as the higher packing density is achieved by solvation.

Bonds in these derivatives, as in other oligoynes,^[19] alternate sharply between triple and single, and show no tendency to equalisation. The butadiyne geometry in **8** is similar to those in recently reported (surprisingly stable) terminal butadiynes.^[29] The phenylene ring shows a quinoidal distortion ($\Delta_{C-C} = 0.023(2)$ Å) similar to that in the planar 4-ethynylaniline molecule^[30] ($\Delta = 0.021(2)$ Å), but only half of that in *p*-nitroaniline.^[31] This may indicate some conjugation be-

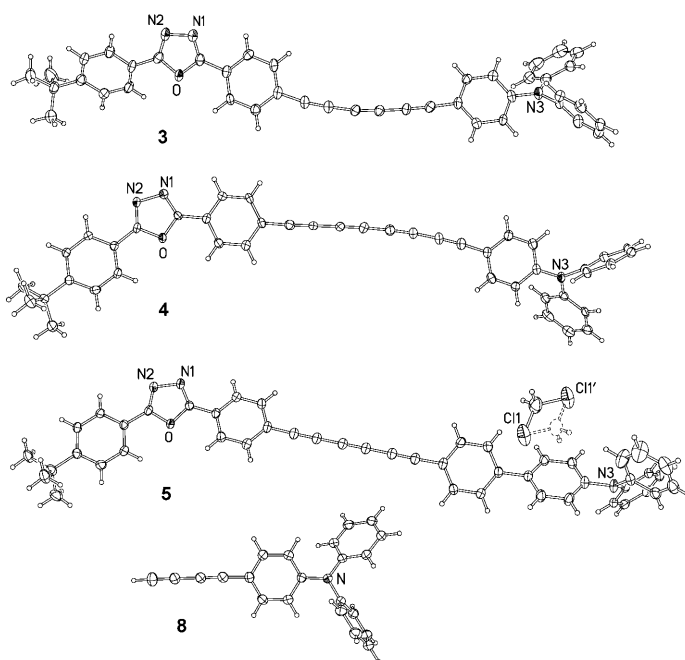


Figure 1. Molecular structures of **3**, **4**, **5**·½ CH₂Cl₂ and **8**, showing 50 % thermal ellipsoids. Minor positions of the disordered CH₂Cl₂ molecule and *t*Bu group in **5** are omitted.

tween the amino and butadiyne substituents, in spite of the 22.5° twist around the N–C(phenylene) bond.

Solution electrochemistry: The solution redox properties of **1**,^[23] **2**,^[23] **3**, **4** and **5** have been studied by cyclic voltammetry (CV) (Figure 2). As expected, the CVs of these compounds are characterised by oxidation and reduction waves due to the triarylamine and oxadiazole moieties, respectively. These are irreversible waves except for the reduction of **1** that is quasi-reversible. In addition, for **2–5** irreversible reduction waves associated with the oligoyne bridges are observed at more negative potentials. The difference between the first oxidation and the first reduction potentials,

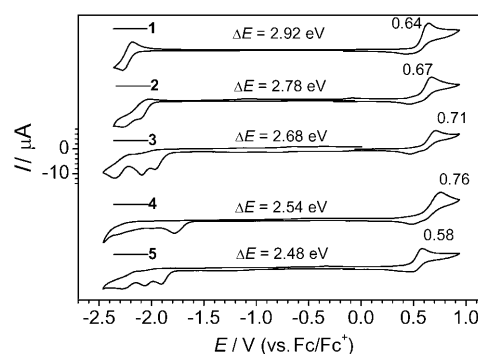


Figure 2. Cyclic voltammograms of compounds **1–5** in MeCN. All solutions contained tetrabutylammonium hexafluorophosphate (TBAPF₆, 0.1 M) as the supporting electrolyte, scan rate 100 mV s^{−1}, using Pt disk ($\Phi = 1.8$ mm) as the working electrode, Pt wire as the counter electrode and Ag/AgNO₃/DMF as the reference electrode.

$E^{\text{ox1}} - E^{\text{red1}}$, is a measure of the HOMO–LUMO gap. A notable trend in Figure 2 is a reduction in the HOMO–LUMO gap in the series of compounds **1–4** as the oligoyne chain length increases, which is consistent with extended conjugation through the elongated bridges. A similar trend was noted in the CV data of two Zn-porphyrin–(C≡C)_n–C₆₀ dyads ($n=1, 2$) studied previously.^[20] Interestingly, an increment of +30 to +50 mV in the value of E^{ox} was observed with each additional triple bond for compounds **1–4**. As noted previously for **1** and **2**,^[23] and for some oligoyne-bridged binuclear organometallic compounds,^[32,33] this can be ascribed to the electron-withdrawing nature of the extra triple bond. In the present D–(C≡C)_n–A systems we cannot exclude the possibility that charge delocalisation across the bridge might play a role in causing these anodic shifts. Compound **5** has the lowest oxidation potential and this may be due to the biphenyl system interrupting conjugation with the electron-withdrawing oligoyne bridge. However, the irreversibility of the waves for **1–5** means that only tentative conclusions should be drawn from the CV data. It can be noted that there is a sequential decrease in the potential of the irreversible oxidation waves of the triarylamine building blocks **6**, **8** and **14** (see Figure S1 in the Supporting Information). This is not a case of electron transfer along the lines of classical Marcus theory, rather it is intramolecular charge transfer (CT), so it is not appropriate to analyse the data by using the Weller equation.

Photophysical studies: Table 1 summarises the absorption and emission data (when observed) and the Stokes shift (when observed) of **1–5** in methylcyclohexane (MCH) as obtained from the data shown for **1**, **2**, **3** and **5** shown in Figure 3. The data are extracted from the lowest energy absorption band (or shoulder) and the sharp peak in the emission spectra. The obtained Stokes shifts show a clear decrease as the conjugation is extended along the series from one to three alkyne units, that is, compounds **1**, **2** and **3**, respectively. We note that this is likely to be an underestimate as different rotational conformations also contribute. The data does, however, imply that as the electronic system becomes more conjugated there is less displacement of the excited-state potential energy curve relative to the ground state.

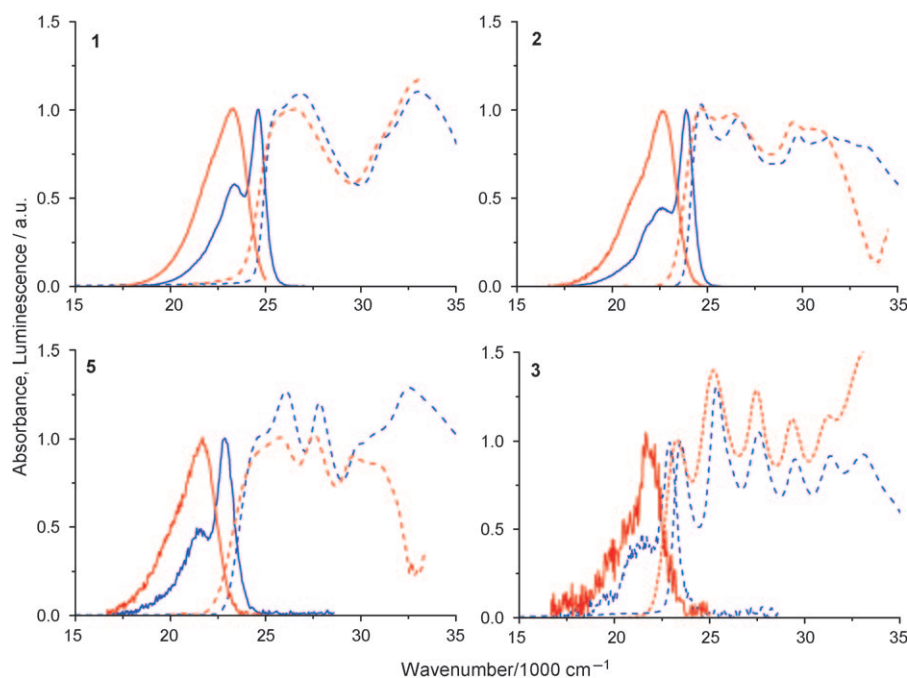


Figure 3. Absorption (dashed line) and luminescence (solid line) spectra for **1**, **2**, **3** and **5** in methylcyclohexane (blue) and toluene (red); excitation at 390 nm (25641 cm^{−1}).

Table 1. Data on the optical transitions of compounds **1–5**.

	$\tilde{\nu}_{\text{abs}}$ [cm ^{−1}]	$\tilde{\nu}_{\text{em}}$ [cm ^{−1}]	$\Delta\tilde{\nu}^{[b]}$ [cm ^{−1}]	μ_{g} [D] AM1 ^[c]	μ_{g} [D] PM3 ^[c]	$\Delta\mu$ [D] ^[d]	μ_{e} [D] ^[e] AM1	μ_{e} [D] ^[d] PM3
1	25575 ^[a]	24570 ^[a]	1005 ^[a]	4.91	4.68	3.2 ± 0.1	8.1 ± 0.1	7.9 ± 0.1
2	24631 ^[a]	23866 ^[a]	764 ^[a]	5.26	5.15	3.9 ± 0.2	9.2 ± 0.2	9.1 ± 0.2
3	23474 ^[a]	22936 ^[a]	538 ^[a]	4.15	4.15	4.3 ± 0.3	8.5 ± 0.3	8.5 ± 0.3
4	21740 ^[a]	–	–	4.27	4.64	–	–	–
5	24450 ^[a]	22830	1620 ^[a]	4.08	4.79	4.9 ± 0.3	9.0 ± 0.2	9.7 ± 0.2

[a] Recorded in a non-polar solvent (methylcyclohexane). [b] $\Delta\tilde{\nu} = \tilde{\nu}_{\text{abs}} - \tilde{\nu}_{\text{em}}$. [c] AM1 and PM3 are the two semiempirical calculation methods used. [d] $\Delta\mu$ according to Equation (2). The luminescence of **3** was recorded with relatively large slit widths (≈ 10 nm) of the spectrometer. Accordingly, the centre of weight of the luminescence is poorly defined, which prevents an accurate calculation of the Stokes shift and thus $\Delta\mu$. [e] Excited-state dipole moment μ_{e} calculated from the ground-state dipole moment and the difference dipole moment: $\mu_{\text{e}} = \mu_{\text{g}} + \Delta\mu$.

The efficiency of intramolecular charge transfer (ICT) in D–A dyads can be examined through optical absorption and emission experiments in media with different solvent polarity. In a low polarity solvent with a solvent density parameter of $\Delta f = 0$, where Δf is defined by Equation (1):

$$\Delta f = \left(\frac{\epsilon_r - 1}{2\epsilon_r + 1} - \frac{n_D^2 - 1}{2n_D^2 + 1} \right) \quad (1)$$

where ϵ_r is the dielectric constant and n_D is the refractive index, the luminescence spectra of **1**, **2**, **3** and **5** in MCH (Figure 3) consist of two distinct features—a sharp and narrow band followed by a considerably broader and gener-

ally structureless component at lower energy. Interestingly, for all other solvents (dielectric medium) where $\Delta f > 0$, the narrow high energy component is no longer observed and the luminescence gives only a broader band devoid of any fine structure. This is demonstrated in Figure 3 that shows the photoluminescence (PL) in two different environments, MCH and toluene. With respect to Equation (1), the solvent density parameter is $\Delta f = 0$ for MCH, whereas $\Delta f = 0.013$ for toluene. This observation indicates how sensitive the excited state is to the environment and how a very small change to more polar media will stabilise the CT state. It is, therefore, clear that for low polarity media with $\Delta f = 0$ the luminescence is due to two different contributions, namely a higher energy narrow band caused by singlet fluorescence ($\pi^* \rightarrow \pi$) and a broader lower energy ICT band. The existence of these two states was suggested by Khundkar et al.^[34a,b] in studies of asymmetrically end-capped diphenylethyne and diphenylbutadiyne molecules—the singlet excited state has also been referred to as a locally excited (LE) state—although the LE state eluded detection in that study.

The hypothesis that the lower energy band is due to ICT is strengthened by absorption and emission experiments on the solvatochromism of **1**, **2**, **3** and **5**, by using a number of solvents with varying polarity, as defined by the solvent density parameter [Eq. (1)]. The data give an apparent Stokes shift $\Delta\tilde{\nu} = \tilde{\nu}_{\max}^{\text{abs}} - \tilde{\nu}_{\max}^{\text{em}}$, where the Stokes shift is now calculated from the lowest energy band in the absorption and the centre of weight of the CT emission. Figure 4 shows the Stokes shift for **1**, **2**, **3** and **5** in various dielectric media. These experiments reveal that there is a moderate impact

on the centre of weight of the absorption while the luminescence centre of weight is substantially more affected by the polarity of the medium. This in turn suggests that the ground-state dipole moment is largely unaffected, in contrast to the excited-state dipole moment that is considerably more sensitive to the medium. Semiempirical calculations (by using two different methods, see Table 1) show that the ground-state dipole moment is approximately 4–5 D and independent of the extent of conjugation, that is, the number of alkyne units in the bridge. This, in turn, implies that when the D–A separation increases there is a slightly less charge localisation in the ground state for the longer, more conjugated compounds. The luminescence is, however, strongly dependent upon the properties of the dielectric medium and considerable bathochromic shifts of the PL centre of weight with a more polar solvent are observed. The experimental observations were analysed by using the Lippert–Mataga–Oshika formalism [Eq. (2)],^[35]

$$\Delta\tilde{\nu} = \tilde{\nu}_{\max}^{\text{abs}} - \tilde{\nu}_{\max}^{\text{em}} = \frac{2(\mu_e - \mu_g)^2}{hca^3} \left(\frac{\epsilon_r - 1}{2\epsilon_r + 1} - \frac{n_D^2 - 1}{2n_D^2 + 1} \right) + \text{constant} \quad (2)$$

which relates the optical properties in various media to the difference dipole moment $\Delta\mu = \mu_e - \mu_g$ and the radius of the Onsager cavity, a . As shown in Figure 4, plots of the Stokes shift $\Delta\tilde{\nu}$ against the solvent density parameter Δf for the compounds **1**, **2**, **3** and **5** results in a linear dependence as would be expected from the Lippert–Mataga–Oshika formalism.

From the slope of the linear fits the difference dipole moment $\Delta\mu = \mu_e - \mu_g$ can be obtained from an estimate of the Onsager radius a . In estimating this radius we used bond lengths and dihedral angles obtained from the X-ray crystal structures. We acknowledge that assuming a spherical volume for these molecules is an approximation; however, we are not aware of any other way forward in this context.

The excited-state dipole moments calculated here are similar to those reported by Stiegman et al. for this type of D–A system.^[36] However, we find that the difference dipole moment is larger for the more conjugated molecules **3** and **5**. This observation is in contrast to Stiegman et al., who observed a reduction in the difference dipole moment for diphenylbutadiynyl D– π –A dyads

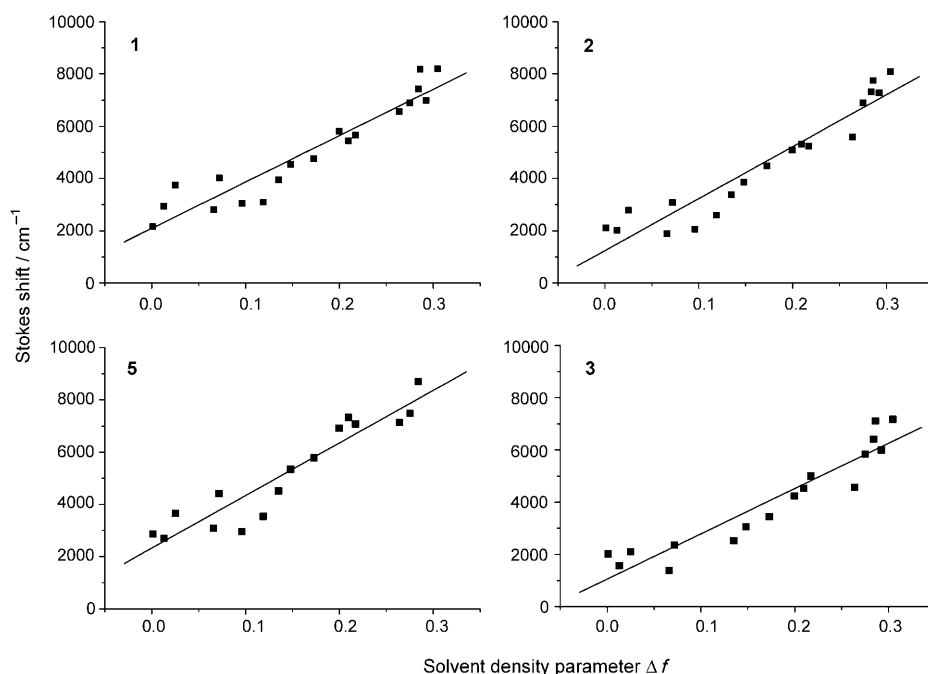


Figure 4. Stokes shifts for **1**, **2**, **3** and **5** as a function of solvent density parameter as defined in Equation (1). The line represents a fit of the data according to the Lippert–Mataga–Oshika relationship as defined in Equation (2) by using a linear regression fit. The quality of the fit is judged by the corresponding R values, which are as follows: **1**: $R = 0.95$, **2**: $R = 0.96$, **3**: $R = 0.95$, **5**: $R = 0.94$.

(D-C₆H₄-(C≡C)_n-C₆H₄-A, *n*=2) compared to diphenylethynyl analogues (*n*=1). This is significant as a relatively smaller excited dipole moment is indicative of less extensive ICT. The data obtained in the present study do, however, show that for these compounds ICT is equally efficient for the more conjugated longer molecules.

Khundkar et al. observed that when the ethynylene bridge was replaced by a butadiynylene bridge in compounds with the same donor and acceptor moieties (i.e., MeS-C₆H₄-(C≡C)_n-C₆H₄-CN, *n*=1, 2) there was a substantial reduction in the PLQY.^[34b] The present series of compounds shows similar behaviour with a dramatic drop in PLQY from 93 % for **1** to 1 % for **3** (Table 2). Insertion of a phenyl ring in **5** results in a slight increase in PLQY although the value remains very low. We note that **4** appears to be luminescent, although the PLQY is extremely low, about 10⁻³.

Table 2. PLQY values and σ_2 data for **1**–**5**.

	PLQY ^[a]		σ_2 [GM]	
	MCH	acetone	MCH	Acetone
1	0.93	0.56	50 ± 10	150 ± 10
2	0.36	0.28	140 ± 10	200 ± 10
3	0.01	0.01	190 ± 50	590 ± 100
4	≈ 10 ⁻³	–	–	–
5	0.04	–	–	–

[a] PLQY values were measured in two different solvents based upon the absolute method by using an integrating sphere (MCH = methylcyclohexane). Errors ± 5 %. The two photon absorption (TPA) cross-sections (σ_2) were measured by using fluorescein/NaOH as a standard (PLQY = 0.9 and σ_2 = 36 GM at λ_{exc} = 800 nm). The concentrations of the standard (fluorescein) was, $c^R = 5 \times 10^{-6}$ M and the concentration of the samples typically $c^S \approx 10^{-6}$ M. See the Supporting Information for more information.

To gain further insights into the optoelectronic properties we also performed two photon absorption (TPA) measurements on **1**, **2** and **3**. Seminal work by Albota et al. clearly suggest that introduction of charge-transfer moieties and extended conjugation of the π -electron system are prerequisites for high TPA cross sections.^[37] It was, therefore, most relevant to examine **1**, **2** and **3** in different dielectric media to assess the impact of conjugation within the homologous series. All three compounds exhibited clear and well-defined TPA PL for excitation at 790 nm, similar in shape to the corresponding linear one photon excited PL spectra with respect to centre of weight of bands (see Figure S3 in the Supporting Information). One difference that could be observed was that the relative intensity of the LE state emission (in methylcyclohexane) is slightly lower relative to the lower energy CT bands. This may be a reflection of different symmetry implications of the TPA process. To examine the effect of changing the dielectric medium, the data for **1**, **2** and **3** were obtained in a non-polar solvent MCH ($\Delta f = 0$) and acetone ($\Delta f = 0.355$), which was the most polar medium in which the compounds were soluble. The data shown in Table 2 clearly show that the TPA cross sections increase significantly for both **1** and **3** with increased polarity of the solvent. At present it is not clear why compound **2** shows a

smaller relative increase in changing from a non-polar to a polar dielectric medium, compared to **1** and **3**. The polar solvents will stabilise the structure of the excited state in favour of a CT state over an LE state. This, in turn, has symmetry implications with possible conformation alterations that explain the enhanced TPA cross sections in polar media. In this context, it is necessary to make additional comments about the PLQY of these compounds. The data show that the PLQY is not only affected by conjugation (as previously discussed) but also by the properties of the dielectric medium. For **1** and **2**, there is a clear decrease of the PLQY in more polar media, as compared to MCH (Table 2). We observed this trend for a number of other more polar solvents. However, there was no systematic variation of PLQY versus solvent density parameter (data not shown). The impact of the medium on the PLQY of **3** is more difficult to assess as the PLQY value is low. In parallel to the effect of the medium on the TPA cross sections, there is also an effect due to increased conjugation. Compound **3**, with the more extended conjugation, also shows the largest TPA cross sections, as expected.^[37] (Note that although σ_2 for **3** is high, there is also a large associated error due to an uncertainty in the PLQY value, as previously discussed).

The luminescence decay of the excited state was also affected by the extent of conjugation through oligoynes bridging (Figure 5). For **1** in a non-polar medium the decay was dominated by a 1.1 ns component, while data for **2** was dominated by an approximate 500 ps component. For the more conjugated compounds **3** and **5** the luminescence decay was very fast and most likely not fully resolved due to insufficient time resolution of the detection system. Accordingly, the time constants for **3** and **5** (Table 3) are somewhat uncertain. In a polar environment a longer decay phase was observed for all four compounds. This supports the suggestion that the luminescence in polar media originates from an ICT state for which longer decay times are expected.^[38] We are confident that there is no degradation of the compounds in chloroform as the PL spectra of **1** and **2** are similar to those in other polar environments.^[23] We note that the luminescence decays appear to be independent of the excitation wavelength. Essentially similar kinetics were obtained for excitation at 300 nm and 400 nm. There were only moderate variations of the PL dynamics with different detection wavelength (in the PL spectra), within the time resolution of our time-correlated single photon counting (TCSPC) apparatus. However, we cannot rule the presence of PL decay phases in the 10⁻¹²–10⁻¹³ s range that would escape detection in our TCSPC system. In combination, the PLQY data and the luminescence decay data reveal that for the more conjugated systems **3** and **5** the excited-state decay is dominated by non-radiative processes. Probing the excited-state decay with transient absorption spectroscopy supports this conclusion. Figure 6 shows pump-probe absorption data for **1**, **2**, **3** and **4** in MCH at 390 nm after excitation with optical pulses with a temporal width of 200 fs.

All the systems studied have an initial fast decay to a longer-lived state, which is estimated to have a lifetime of

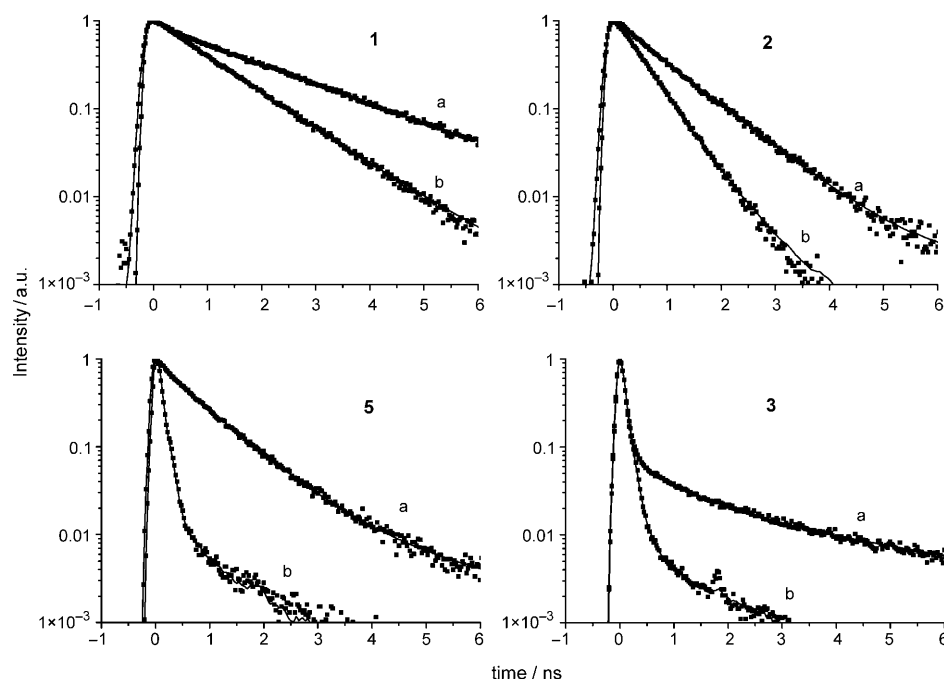


Figure 5. Luminescence decays recorded in the emission maxima of compounds **1**, **2**, **3** and **5**. Data recorded in polar solvent (rigorously purified chloroform: data points a) and a non-polar solvent (methylcyclohexane: data points b). Excitation wavelength $\lambda_{\text{ex}} = 295$ nm. See text and the Supporting Information for details of the data analysis.

Table 3. Data obtained in time domain experiments. Luminescence decay data were obtained in TCSPC experiments.

	Lum. decay (MCH) ^[a]		Lum. decay (CHCl ₃) ^[b]		Pump-probe abs. (MCH) ^[a]		ΔE [eV]
	τ_1 [ns]	τ_2 [ns]	τ_1 [ns]	τ_2 [ns]	τ_1 [ns]	τ_2 [ns]	
1	1.0	—	0.2 (10 %)	2.0 (90 %)	0.78	—	3.17
2	0.5	—	0.1 (5 %)	1.0 (95 %)	0.35 (50 %)	≈ 15 (50 %)	3.05
3	≈ 0.06	—	0.1 (5 %)	1.0 (95 %)	0.30 (50 %)	≈ 10 (50 %)	2.91
4	—	—	—	—	0.03 (50 %)	≈ 10 (50 %)	2.71
5	≈ 0.06	—	0.15 (5 %)	1.0 (95 %)	—	—	—

[a] MCH = methylcyclohexane. [b] Percentage number in brackets is the relative contribution of the particular decay phase. The energy gap is taken as the lowest energy absorbing species in the absorption spectrum. See text for details.

tens of ns. We note that there was no corresponding decay time found in the luminescence experiments. However, the same trend as in the time-resolved PL experiments was observed in the ultrafast transient absorption. This trend shows that the absorption recovery time of the first component becomes faster with increasing length of the oligoene bridge, that is, increasing conjugation (see Table 3). The PL dynamics are, therefore, limited by the excited-state lifetime. The excited-state decay, as monitored in the transient absorption measurements in a non-polar medium is, therefore, due to two phases: a fast direct relaxation from the excited state to the ground state, or via a charge separated state that will recombine non-radiatively on relatively slower timescales compared to the PL dynamics. In order to learn more about the nature of the slow ns component observed in the transi-

ent absorption measurements (Figure 6 and Table 3), additional experiments were performed on **3** and **4**, where this phase is more prominent. Excited-state absorption experiments revealed a strong absorption at approximately 470 nm for both **3** and **4** (see the Supporting Information for details). Probing the decay dynamics of this band at 470 nm did not result in any detected transient species. The reason for this is the time resolution of our experimental apparatus that is in the order of ≈ 70 ns. Hence, the recovery in this band must be in the ≈ 10 ns range. Interestingly, when the probe wavelength was 639 nm recovery to the ground state was sufficiently slow to be monitored. Furthermore, the decay dynamics of this species showed a marked sensitivity to the presence of oxygen. Hence, we conclude that this absorption is due to triplet-triplet absorption. It then remains to assign the strong band around 470 nm to excited-state absorption of a dark charge-transfer state with a lifetime in the ns regime as no corresponding decay phase was observed in the time-resolved PL experiments as previously mentioned.^[39] This conclusion correlates well with the observation of fast luminescence dynamics observed for **3** (see Figure 5).

The initial faster decay shows interesting behaviour depending on the length of the oligoene bridge. This aspect will now be discussed in more detail. Compound **1**, with the shortest bridge, exhibits a slow decay of the luminescence in conjunction with a slow return to the ground state in the transient absorption measurements. For the more extended analogues **2**, **3** and **4** the kinetics become faster in both luminescence and transient absorption (Table 3). In conjunction with the PLQY data, the scenario is, therefore, that strong non-radiative pathways dominate the excited-state decay for more conjugated systems. The same phenomena have been observed experimentally for a number of related systems.^[40] The mechanism behind the non-radiative decay has not yet been clarified but the possibility that the non-radiative relaxation is connected to the ground- and excited-state energy gap has been

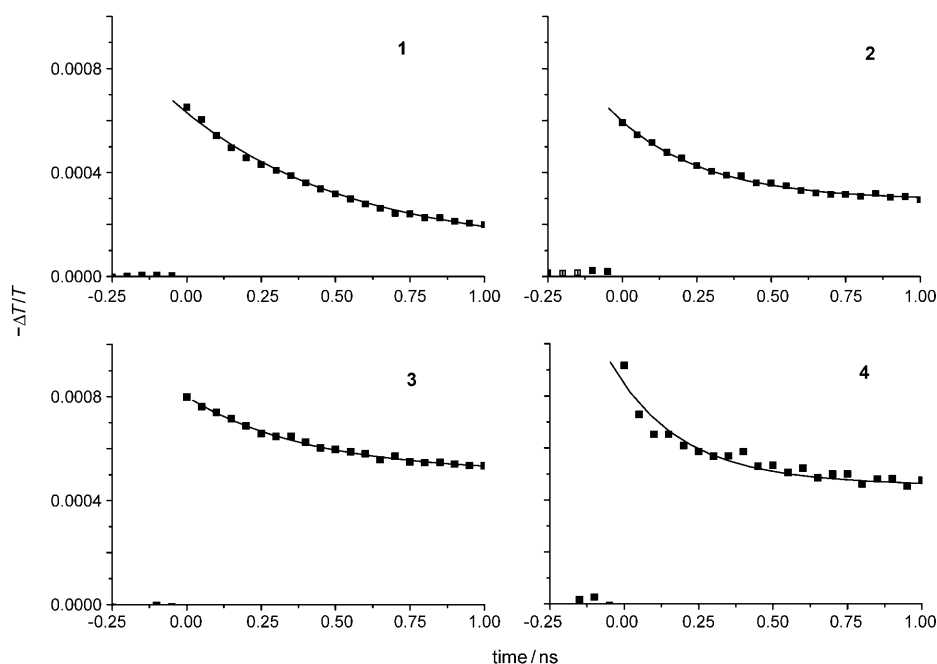


Figure 6. Ambient temperature transient absorption data for **1**, **2**, **3** and **4** for excitation and probing at 390 nm in MCH. The squares represent the measured data and the line is the fit of the data. See text for details.

considered.^[36] This dependency is commonly known as the energy-gap law and the framework was outlined by Engelman and Jortner in the 1970s.^[24] This law defines two limiting cases, referred to as the strong and weak coupling limits, which in turn relate to the extent of displacement of the LUMO relative to the HOMO potential energy surface. In the case of the weak coupling limit, the reorganisation energy (λ) is considered to be small and it also assumes a moderate temperature-dependence of the PLQY, which was observed for the present series of compounds (see the Supporting Information for details). Prominent factors in the weak coupling limit are high frequency vibrational modes, which are common for organic-based materials. For the strong coupling limit on the other hand, the potential surfaces of the ground and excited state are identical. The strong coupling case implies that the Stokes shift considerably exceeds the mean vibrational frequency.^[24] From the recorded Stokes shifts (Table 1) we conclude that those are likely to be significantly less than the energies of prominent vibrational modes of the systems studied here.

Assuming that the weak coupling limit is valid in this case, the non-radiative decay rate k_{nr} is then given by Equation (3):^[36,40]

$$k_{nr} = \frac{V^2(2\pi)^{\frac{1}{2}}}{\hbar(\hbar\omega_M\Delta E)^{\frac{1}{2}}} \cdot \exp\left[-\frac{\lambda}{\hbar\omega_M}\right] \cdot \exp\left[-\frac{\gamma\Delta E}{\hbar\omega_M}\right] \quad (3)$$

In this formalism V is the electronic coupling between the ground and excited state, ΔE represents the energy gap (LUMO–HOMO), ω_M is the vibrational frequency and γ is an analytical function which contains structural information.

The reorganisation energy λ must be equal to, or less than, the average vibrational energy $\hbar\omega_{ave}$. For the systems studied here prominent modes are the C=C stretch vibration at $\tilde{\nu} \approx 1600 \text{ cm}^{-1}$, the C≡C stretch vibration at $\tilde{\nu} \approx 2200 \text{ cm}^{-1}$ and the C–H stretch vibration at $\tilde{\nu} \approx 3000 \text{ cm}^{-1}$. We remark that the energy in all these vibrations exceeds the reorganisation energy as estimated from the Stokes shift obtained from the lowest energy band in the absorption spectra and the sharp LE emission (see Figure 1 and Table 1).

In Equation (3) the parameter γ depends only weakly on the energy gap ΔE and the analytical expression for γ is given by Equation (4):^[36]

$$\gamma = \ln\left(\frac{2\Delta E}{n\hbar\omega_M\Delta Q^2}\right) - 1 \quad (4)$$

where ΔQ is the average displacement between the ground- and excited-state potential energy surfaces. Taking the natural logarithm of Equation (3) gives Equation (5).

$$\ln k_{nr} \propto -\frac{1}{2}\ln \Delta E - \gamma \frac{\Delta E}{\hbar\omega_M} \quad (5)$$

This is more useful as there is a linear relationship between $\ln k_{nr}$ and ΔE . Furthermore, the logarithmic term in Equation (5) contributes only marginally to the dependence of ΔE on $\ln k_{nr}$. Consequently, the pre-exponential factor in Equation (3) can be regarded as a constant and with these approximations the relationship shown in Equation (6) is obtained where C is the constant term:

$$\ln k_{nr} \approx C\gamma \frac{\Delta E}{\hbar\omega_M} \quad (6)$$

Figure 7 displays the results obtained for compounds **1**, **2**, **3** and **4** where the length of the oligoyne bridge is systematically extended. The data fit reasonably well to a linear dependence, as would be expected from Equation (6) and thus, confirm a weak coupling behaviour as outlined previously.

A significant difference between D– π –A systems with oligoene bridges^[18d] and the oligoynes in the present study is that the oligoynes display the energy gap law dependence while the oligoenes do not. This could be due to prevention of isomerisation processes after excitation of the oligoynes

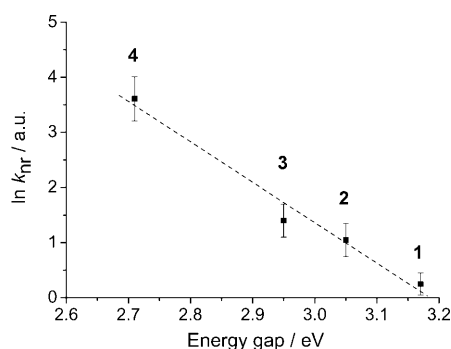


Figure 7. The non-radiative decay rates for **1**, **2**, **3** and **4** plotted against the energy gap. The dashed line indicates a linear trend of the data. See text for details.

due to the unique structure of the triple bond, which upon excitation remains conformationally locked in a structure similar to a double bond. In contrast, excitation of oligoenes may lead to extensive isomerisation processes.^[18d]

Conclusions

We have observed strong solvatochromism of the photoluminescence (PL) of triphenylamine-(C≡C)_n-2,5-diphenyl-1,3,4-oxadiazole systems which points to an efficient intramolecular charge transfer (ICT), even for the longer, more conjugated dyads. Two photon excitation (TPE) PL supports this hypothesis as the TPE cross section was found to be sensitive to the properties of the dielectric medium and the extent of conjugation. The PLQY was observed to be extremely dependent upon the size of the conjugated π -electron system as well as the luminescence decay. This phenomenon has been observed previously for a number of similar systems, but the origin of this effect was not clearly established.^[30] By investigating the excited-state properties of a series of triphenylamine-(C≡C)_n-oxadiazole dyads we have shown that the initial fast excited-state decay is governed by the electronic energy gap law as formulated by the Engelman-Jortner model.^[24] For the present series of dyads we observed ICT and have established that the non-radiative decay is driven by the weak coupling limit. This contrasts with the Zn-porphyrin-(C≡C)_n-C₆₀ dyads ($n=1-4$)^[20] that possess stronger electron donor and acceptor moieties and exhibit classical Marcus behaviour, that is, electron transfer with a very small attenuation factor (β). The present study is among the most comprehensive reported to date^[20] on the optoelectronic properties of molecules bridged by oligoynes units and should stimulate further work on electronic interactions mediated by oligoynes bridges.

Acknowledgements

C.S.W. was funded by EPSRC. L.O.P. acknowledges financial support from CENAMPS. We thank Professor J. A. K. Howard for providing the

X-ray facilities and EPSRC for funding the improvement to the X-ray instrumentation.

- [1] a) *Electron Transfer in Chemistry* (Ed.: V. Balzani), Wiley-VCH, Weinheim, **2001**; b) D. M. Adams, L. Brus, C. E. D. Chidsey, S. Greager, C. Creutz, C. R. Kagan, P. V. Kamat, M. Lieberman, S. Lindsay, R. A. Marcus, R. M. Metzger, M. E. Michel-Beyerle, J. R. Miller, M. D. Newton, D. R. Rolison, O. Sankey, K. S. Schanze, J. Yardley, X. Zhu, *J. Phys. Chem. B* **2003**, *107*, 6668–6697; c) E. A. Weiss, M. R. Wasielewski, M. A. Ratner, *Top. Curr. Chem.* **2005**, *257*, 103–133.
- [2] Reviews on molecular electronics: a) R. L. Carroll, C. B. Gorman, *Angew. Chem.* **2002**, *114*, 4556–4579; *Angew. Chem. Int. Ed.* **2002**, *41*, 4378–4400; b) A. C. Benniston, *Chem. Soc. Rev.* **2004**, *33*, 573–578; c) G. R. Maruccio, R. Cingolani, R. Rinaldi, *J. Mater. Chem.* **2004**, *14*, 542–554; d) A. Troisi, M. A. Ratner, *Small* **2006**, *2*, 172–181.
- [3] a) H. Oevering, M. N. Paddon-Row, M. Heppener, A. M. Oliver, E. Cotsaris, J. W. Verhoeven, N. S. Hush, *J. Am. Chem. Soc.* **1987**, *109*, 3258–3269; b) M. R. Wasielewski, *J. Org. Chem.* **2006**, *71*, 5051–5066.
- [4] Review: B. Albinsson, M. P. Eng, K. Pettersson, M. U. Winters, *Phys. Chem. Chem. Phys.* **2007**, *9*, 5847–5864.
- [5] a) P. J. Low, *Dalton Trans.* **2005**, 2821–2824; b) A. C. Benniston, A. Harriman, *Coord. Chem. Rev.* **2008**, *252*, 1268–1277.
- [6] *Electronic Materials: The Oligomer Approach* (Eds.: G. Wegner, K. Müllen), Wiley-VCH, Weinheim, **1998**.
- [7] a) F. Giacalone, J. L. Segura, N. Martín, D. M. Guldi, *J. Am. Chem. Soc.* **2004**, *126*, 5340–5341.
- [8] a) M. Irie, *Chem. Rev.* **2000**, *100*, 1685–1716; b) D. Gust, T. A. Moore, A. L. Moore, *Chem. Commun.* **2006**, 1169–1178; c) V. Balzani, A. Credi, M. Venturi, *Molecular Devices and Machines*, Wiley-VCH, Weinheim, **2008**.
- [9] S. Günes, H. Neugebauer, N. S. Sariciftci, *Chem. Rev.* **2007**, *107*, 1324–1338.
- [10] Y. Shiota, H. Kageyama, *Chem. Rev.* **2007**, *107*, 953–1010.
- [11] J. Zaumseil, H. Sirringhaus, *Chem. Rev.* **2007**, *107*, 1296–1323.
- [12] a) R. L. McCreery, *Chem. Mater.* **2004**, *16*, 4477–4496; b) S. M. Lindsay, M. A. Ratner, *Adv. Mater.* **2007**, *19*, 23–31; c) F. Chen, J. Hihath, Z. Huang, X. Li, N. J. Tao, *Annu. Rev. Phys. Chem.* **2007**, *58*, 535–564.
- [13] E. A. Weiss, M. J. Ahrens, L. E. Sinks, A. V. Gusev, M. A. Ratner, M. R. Wasielewski, *J. Am. Chem. Soc.* **2004**, *126*, 5577–5584.
- [14] a) J. L. Segura, N. Martín, D. M. Guldi, *Chem. Soc. Rev.* **2005**, *34*, 31–47; b) F. Giacalone, J. L. Segura, N. Martín, J. Ramey, D. M. Guldi, *Chem. Eur. J.* **2005**, *11*, 4819–4834.
- [15] a) U. H. F. Bunz, *Chem. Rev.* **2000**, *100*, 1605–1644; b) C. Atienza, B. Insuasty, C. Seoane, N. Martín, J. Ramey, G. M. A. Rahman, D. M. Guldi, *J. Mater. Chem.* **2005**, *15*, 124–132; c) C. Atienza, N. Martín, M. Wielopolski, N. Haworth, T. Clark, D. M. Guldi, *Chem. Commun.* **2006**, 3202–3204; d) K. Pettersson, J. Wiberg, T. Ljungdahl, J. Martensson, B. Albinsson, *J. Phys. Chem. A* **2006**, *110*, 319–326.
- [16] a) R. H. Goldsmith, L. E. Sinks, R. F. Kelley, L. J. Betzen, W. Liu, E. A. Weiss, M. A. Ratner, M. R. Wasielewski, *Proc. Natl. Acad. Sci. USA* **2005**, *102*, 3540–3545; b) C. Atienza-Castellanos, M. Wielopolski, D. M. Guldi, C. van der Pol, M. R. Bryce, S. Filippone, N. Martín, *Chem. Commun.* **2007**, 5164–5166; c) R. H. Goldsmith, O. DeLeon, T. M. Wilson, D. Finkelstein-Shapiro, M. A. Ratner, M. R. Wasielewski, *J. Phys. Chem. A* **2008**, *112*, 4410–4414.
- [17] T. Otsubo, Y. Aso, K. Takimiya, *J. Mater. Chem.* **2002**, *12*, 2565–2575.
- [18] a) T. S. Arrhenius, M. Blanchard-Desce, M. Dvornitzky, J. M. Lehn, J. Malthete, *Proc. Natl. Acad. Sci. USA* **1986**, *83*, 5355–5359; b) M. C. Díaz, M. A. Herranz, B. M. Illescas, N. Martín, N. Godbert, M. R. Bryce, C. Luo, A. Swartz, G. Andersen, D. M. Guldi, *J. Org. Chem.* **2003**, *68*, 7711–7721; c) F. He, F. Chen, J. Li, O. F. Sankey, Y. Terazono, C. Herrero, D. Gust, T. A. Moore, A. L. Moore, S. M.

- Lindsay, *J. Am. Chem. Soc.* **2005**, *127*, 1384–1385; d) W. Akemann, W. Laage, P. Plaza, M. M. Martin, M. Blanchard-Desce, *J. Phys. Chem. B* **2008**, *112*, 358–368.
- [19] a) S. Szafert, J. A. Gladysz, *Chem. Rev.* **2003**, *103*, 4175–4205; b) S. Szafert, J. A. Gladysz, *Chem. Rev.* **2006**, *106*, PR1–PR33; c) T. Gibner, F. Hampel, J. P. Gisselbrecht, A. Hirsch, *Chem. Eur. J.* **2002**, *8*, 408–432; d) Y. Morisaki, T. Luu, R. R. Tykwinski, *Org. Lett.* **2006**, *8*, 689–692; e) J. Kendall, R. McDonald, M. J. Ferguson, R. R. Tykwinski, *Org. Lett.* **2008**, *10*, 2163–2166.
- [20] S. A. Vail, P. J. Krawczuk, D. M. Guldi, A. Palkar, L. Echegoyen, J. P. C. Tomé, M. A. Fazio, D. I. Schuster, *Chem. Eur. J.* **2005**, *11*, 3375–3388.
- [21] a) J. Taylor, M. Brandbyge, K. Stokbro, *Phys. Rev. B* **2003**, *68*, 121101; b) P. V. James, P. K. Sudeep, C. H. Suresh, K. G. Thomas, *J. Phys. Chem. A* **2006**, *110*, 4329–4337.
- [22] a) A. D. Slepko, F. A. Hegmann, S. Eisler, E. Elliott, R. R. Tykwinski, *J. Chem. Phys. B* **2004**, *120*, 6807–6810; b) S. Eisler, A. D. Slepko, E. Elliott, T. Luu, R. McDonald, F. A. Hegmann, R. R. Tykwinski, *J. Am. Chem. Soc.* **2005**, *127*, 2666–2676.
- [23] C. Wang, L.-O. Pålsson, A. S. Batsanov, M. R. Bryce, *J. Am. Chem. Soc.* **2006**, *128*, 3789–3799.
- [24] a) R. Engelman, J. Jortner, *J. Mol. Phys.* **1970**, *18*, 145–164; b) K. F. Freed, J. Jortner, *J. Chem. Phys.* **1970**, *52*, 6272–6291.
- [25] S. Gauthier, J. M. J. Frechet, *Synthesis* **1987**, 383–385.
- [26] a) D. E. Ames, D. Bull, C. Takunda, *Synthesis* **1981**, 364–365; b) Z. Novák, P. Nemes, A. Kotschy, *Org. Lett.* **2004**, *6*, 4917–4920.
- [27] November 2008 issue of Cambridge Structural Database, see: F. H. Allen, R. Taylor, *Chem. Soc. Rev.* **2004**, *33*, 463–475.
- [28] R. Dembinski, T. Lis, S. Szafert, C. L. Mayne, T. Bartik, J. A. Gladysz, *J. Organomet. Chem.* **1999**, *578*, 229–246.
- [29] a) K. West, C. Wang, A. S. Batsanov, M. R. Bryce, *J. Org. Chem.* **2006**, *71*, 8541–8544; b) K. West, C. Wang, A. S. Batsanov, M. R. Bryce, *Org. Biomol. Chem.* **2008**, *6*, 1934–1937; c) K. West, L. N. Hayward, A. S. Batsanov, M. R. Bryce, *Eur. J. Org. Chem.* **2008**, 5093–5098; d) C. Wang, A. S. Batsanov, K. West, M. R. Bryce, *Org. Lett.* **2008**, *10*, 3069–3072.
- [30] A. Dey, R. K. R. Jetti, R. Bose, G. R. Desiraju, *CrystEngComm* **2003**, *5*, 248–252.
- [31] M. Tonogaki, T. Kawata, S. Ohba, Y. Iwata, T. Shibuya, *Acta Crystallogr. Sect. B* **1993**, *49*, 1031–1039.
- [32] G.-L. Xu, C.-Y. Wang, Y.-H. Ni, T. G. Goodson III, T. Ren, *Organometallics* **2005**, *24*, 3247–3254.
- [33] For analysis of the redox properties of symmetrical organometallic-capped oligoynes chains, see: a) M. Brady, W. Weng, Y. Zhou, J. W. Seyler, A. J. Amoroso, A. M. Arif, M. Böhme, G. Frenking, J. A. Gladysz, *J. Am. Chem. Soc.* **1997**, *119*, 775–788; b) R. Dembinski, T. Bartik, B. Bartik, M. Jaeger, J. A. Gladysz, *J. Am. Chem. Soc.* **2000**, *122*, 810–822.
- [34] a) L. R. Khundkar, J. T. Bartlett, M. Biswas, *J. Chem. Phys.* **1995**, *102*, 6456–6462; b) M. Biswas, P. Nguyen, T. B. Marder, L. R. Khundkar, *J. Phys. Chem. A* **1997**, *101*, 1689–1695; c) Y. V. Il'ichev, W. Kühnle, K. A. Zachariasse, *J. Phys. Chem. A* **1998**, *102*, 5670–5680; d) K. A. Zachariasse, T. van der Haar, A. Hebecker, U. Leinhos, W. Kühnle, *Pure Appl. Chem.* **1993**, *65*, 1745–1750.
- [35] a) Y. Ooshika, *J. Phys. Soc. Jpn.* **1954**, *9*, 594–601; b) E. Lippert, *Z. Naturforsch. A* **1955**, *10*, 541–545; c) N. Mataga, Y. Kaifu, M. Koizumi, *Bull. Chem. Soc. Jpn.* **1956**, *29*, 465–470.
- [36] A. E. Stiegman, E. Graham, K. J. Perry, L. R. Khundkar, L.-T. Cheng, J. W. Perry, *J. Am. Chem. Soc.* **1991**, *113*, 7658–7666.
- [37] M. Albota, D. Beljonne, J.-L. Brédas, J. E. Ehrlich, J.-Y. Fu, A. A. Heikal, S. E. Hess, T. Kogej, M. D. Levin, S. M. Marder, D. McCord-Maughon, J. W. Perry, H. Röckel, M. Rumi, G. Subramaniam, W. W. Webb, X.-L. Wu, C. Xu, *Science* **1998**, *281*, 1653–1656.
- [38] F. B. Dias, S. Pollock, G. Hedley, L.-O. Pålsson, A. P. Monkman, I. I. Perepichka, I. F. Perepichka, M. Tavasli, M. R. Bryce, *J. Phys. Chem. B* **2006**, *110*, 19329–19339.
- [39] L. R. Khundkar, A. E. Stiegman, J. W. Perry, *J. Phys. Chem.* **1990**, *94*, 1224–1226.
- [40] a) M. Bixon, J. Jortner, J. Cortes, H. Heitele, M. E. Michel-Beyerle, *J. Phys. Chem.* **1994**, *98*, 7289–7299; b) P. O. Andersson, S. M. Bachilo, R.-L. Chen, T. Gillbro, *J. Chem. Phys.* **1995**, *102*–103, 16199–16209.

Received: July 28, 2009

Published online: December 18, 2009